Adsorption of Organic Compounds onto Mineral Substrate Prepared from Oyster Shell Waste

Young-Woong Jeon, Myung-Chan Jo*,
Byeong-Il Noh*, and Choon-Hwan Shin**

Dept. of Environmental Engineering, Kyungpook National University, Taegu, 702-701, Korea
**Dept. of Chemical Engineering, Dongseo University, Pusan 617-716, Korea*
***Dept. of Environmental Engineering, Dongseo University, Pusan 617-716, Korea*

(Manuscript received on March 23, 2001)

Humic acids react with chlorine to produce Trihalomethanes(THMs), known as carcinogens, during disinfection, the last stage in water purification. Currently, the removal of organic humic acids is considered the best approach to solve the problem of THM formation. Accordingly, the current study examined the adsorption of organic compounds of humic acids onto an inorganic carrier prepared from oyster shell waste. The adsorbent used was activated oyster shell powder(HAP) and silver ion-exchanged oyster shell powder(HAP-Ag), with $CaCO_3$ as the control. The adsorbates were phthalic acid, chelidamic acid, catechol, dodecylpyridinium chloride(DP), and 2-ethyl phenol(2-EP).

The adsorption experiments were carried out in a batch shaker at 25 °C for 15 hours. The equilibrium concentration of the adsorbate solution was analyzed using a UV spectrophotometer and the data fitted to the Langmuir isotherm model. Since the solution pH values were found to be greater than the pKa values of the organic compounds used as adsorbates, the compounds apparently existed in ionic form.

The adsorptive affinities of the organic acid and phenolic compounds varied depending on the interaction of electrostatic forces, ion exchange, and chelation. More carboxylic acids and catechol, rather than DP and 2-EP, were adsorbed onto HAP and HAP-Ag. HAP and HAP-Ag exhibited a greater adsorptive affinity for the organic compounds than $CaCO_3$, used as the control.

Key words : humic acids, oyster shell powder, silver ion, ion-exchange, adsorption

1. Introduction

Massive amounts of oyster shell are produced every year as a result of the oyster culturing at Namhae in Korea, a high income fishery business. About 30 % of the oyster shell is reused as fertilizer and feed, while the rest is abandoned as waste[1,2]. Oyster shell waste causes many problems, including coastal pollution and bad smells due to the rotting of the organic substance attached to the shell. In addition, oyster shell is classified as a waste material and its treatment cost is expensive. Consequently, the mass reuse of oyster shell waste is urgent to prevent environmental pollution and reduce waste treatment costs.

The possibility of reusing oyster shell waste as a water treatment agent with both antimicrobial activity and adsorption capacity has already been examined. An antimicrobial water treatment agent is manufactured by crushing oyster shell and exchanging antimicrobial silver ions onto the crushed oyster shell powder. To increase the ion exchange capacity, the oyster shell powder is calcined before the ion exchange process. Among the various antimicrobial metal ions, silver ion was selected for the ion exchange due to its high antimicrobial activity and high selectivity for metal ions on the powder surface. In addition, since the desorption concentration of exchanged silver ion is within the regulation range, it also eliminates the risk of water

pollution while being used as a water treatment agent[3,4].

Chlorine is widely used for disinfection as the last stage in water purification processes. However, chlorine reacts with organic humic acids to produce carcinogenic trihalomethane(THMs), such as chloroform, dibromochloromethane, and bromoform. Ozone has been considered as a substitute disinfectant, yet ozone treatment also produces harmful byproducts and requires high capital and operating costs. Consequently, to provide a secure water supply, the removal of humic acids in water purification processes is thought to be the best method.

In the current study, manufactured oyster shell powder(HAP) and antimicrobial oyster shell powder(HAP-Ag) were used as adsorbents, along with CaCO₃, which is the major component of oyster shell, as the control. The adsorption characteristics of organic compounds onto the adsorbents were investigated. Humic acids were selected as the adsorbates for the adsorption experiment due to the importance of their removal in water purification processes.

2. Materials and Methods

2.1. Characteristics of adsorbates

Humic substances in water include various components and are yellow or black. They are organic substances that contain most of the dissolved organic compounds naturally formed in water and exhibit the general characteristics of functional groups containing many carbons, such as phenolic OH, alcoholic OH, and C=O of quinone. The formation of humic acid is thought to result from a condensation reaction including polyphenol and quinone. From recent reports, it is probable that polyphenol, which originates from lignin and is synthesized by microorganisms, is converted to quinone. There are a number of precursor molecules and formation processes involved in the creation of a humic substance[5].
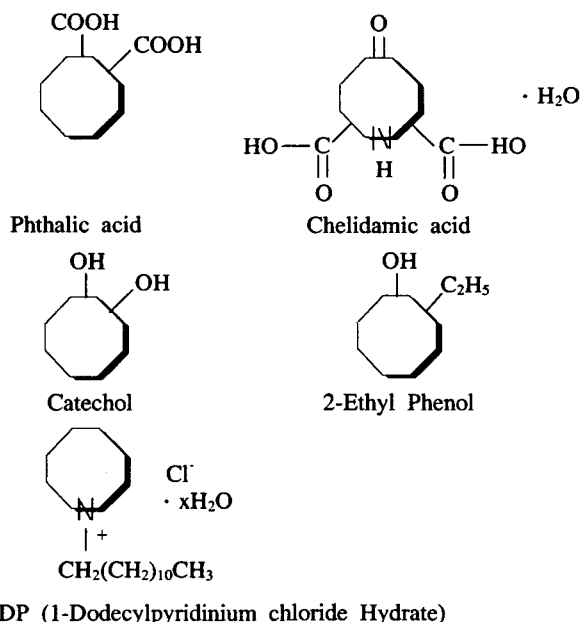
As the adsorbates, five organic compounds, phthalic acid, chelidamic acid monohydrate, catechol, 1-dodecylpyridinium chloride hydrate(DP), and 2-ethyl-phenol(2-EP), were purchased from Aldrich Co. and used for the adsorption experiment. HAP and HAP-Ag were ionized in an aqueous solution so as to be positively charged on their surface due to Ca²⁺, thereby facilitating the negatively charged functional groups of the organic compounds to be adsorbed onto the adsorbent by electrostatic forces, ion exchange, and chelation.

The physical and chemical properties of the organic adsorbates are summarized in Table 1. Fig. 1 shows the molecular structure of the organic adsorbates. As seen in Fig. 1, phthalic acid and chelidamic acid have two -COOH functional groups, while catechol has two -OH functional groups, and DP is a cationic surfactant, while 2-EP is a phenolic compound.

Table 1. Physical and chemical properties of organic adsorbates[8]

Organic Adsorbate	pKa	Molecular Weight	λ_{max}	Purity (%)
Phthalic Acid	2.89	166.13	230	99.5+
Chelidamic Acid	-	201.13	260	97+
Catechol	9.85	110	276	99+
DP	-	283.9	260	98+
2-EP	10.09	122.17	272	99+

DP (1-Dodecylpyridinium chloride Hydrate)

Fig. 1. Molecular structure of organic compounds.

2.2. Adsorption Isotherm

An adsorption isotherm is defined as the relation

in equilibrium between the adsorbate concentration in the solution and the amount of the adsorbate adsorbed on the adsorbent in the solution at a constant temperature. A Langmuir isotherm is usually used to model liquid adsorption and can be expressed by the following equation[6].

$$q = q_m \frac{bc}{1 + bc}$$

where,

q = uptake(adsorbed amount of adsorbate per amount of adsorbent) in equilibrium

q_m = adsorption capacity per amount of adsorbent in equilibrium

b = equilibrium constant depending on temperature

c = equilibrium concentration of adsorbate in solution

In this study, the adsorption data were fitted to this Langmuir isotherm model equation and the characteristics investigated by analyzing the parameter values.

2.3. Manufacture of HAP

Oyster shell produced in Namhae was desalinated by washing with tap water and dried for 3 days in the atmosphere. The dried oyster shell was then crushed by a jaw crusher and calcined at 900 °C for 3 hours to create activation on the surface. The calcined oyster shell was reduced to powder by ball milling and then dried at 110 °C for 24 hours. This activated oyster shell powder was called HAP.

2.4. Manufacture of HAP-Ag

From an XRF analysis, it was found that HAP was mainly composed of SiO_2, Al_2O_3, and CaO. These components can be seen in zeolite with a molecular structure of $XM_{2/n} \cdot Al_2O_3 \cdot YSiO_2 \cdot ZH_2O$, which is a typical inorganic carrier. Although metal ions, such as Na^+ and K^+, are also contained in the zeolite structure, these metal ions do not participate in the formation of the structure itself, but are positioned to maintain the charge balance, thus ion exchange with these ions does not appear to cause any changes in the molecular structure. Therefore, HAP was also expected to be exchangeable with other metal ions due to the

similarity in its molecular structure with zeolite.

To provide antimicrobial activity, an antimicrobial metal ion was exchanged with the metal ions in HAP. Among the various antimicrobial metal ions, silver ion was selected for the ion exchange because of its high selectivity for metal ions with an oxidation number of +1 and high bonding energy with oxygen in a molecular structure to form a stable bond[7].

About 10~40 g of HAP was put in 100~250 ml of deionized water and agitated at 60 °C for 90 minutes. The pH of the solution was controlled at 6.5 using acetic acid. For the ion exchange, 0.339~1.335 g of $AgNO_3$ was dissolved in the solution, which was then agitated for 24 hours. After the ion exchange, the ion-exchanged HAP was separated from the solution by vacuum filtration, washed with deionized water, and dried at 105 °C for 60 minutes. Thereafter, it was crushed and dried again to produce the final antimicrobial water treatment agent(HAP-Ag).

Based on this treatment, it was found that 99.9 % of the silver ion was exchanged in the HAP, plus the desorption concentration of the exchanged silver ion was less than 0.03 %, which is within the regulation range(50 to 100 ppb).

2.5. Adsorption Experiment

To investigate the adsorption characteristics of the organic adsorbates with the adsorbents HAP, HAP-Ag, and $CaCO_3$, batch experiments were conducted. The experimental procedure is described below :

1) 2, 4, 6, 8, 10, 12, 15, 20, 40, 60, 80, and 100 mg/l concentrations of adsorbate solutions were prepared.
2) 3 blanks(1g HAP, HAP-Ag, and $CaCO_3$ + 20 ml distilled water) were prepared.
3) 1 g of HAP, HAP-Ag, and $CaCO_3$ was put in a 50 ml flask, respectively, and solutions of each concentration were poured into the flask. Adsorption was then allowed for 15 hours in a shaking incubator(200 rpm, 25 °C).
4) After precipitation for several hours, a sample of the solution was collected from the top using a syringe and filtered with a 13 mm diameter membrane filter(Pore size 0.2 μ m, Millipore).
5) 5 ml of the filtered solution was diluted 3 times

using distilled water and acidified to the desired pH condition for calibration using 1 N sulfuric acid.

6) The UV absorbency of the pH-controlled sample solution was measured with a specified wavelength using a Diode Array Spectrophotometer(Hewlet Packard 8452A).

7) The uptake(mg adsorbate/g adsorbent) was correlated with the corresponding equilibrium concentration of the adsorbate in solution C(mg adsorbate/l) using a Langmuir isotherm.

2.6. Measurement and Analysis

The thermal behavior of the oyster shell powder was examined by TG/DTA(Thermal Gravimetric /Differential Thermal Analysis) and the phase change according to the calcination temperature was analyzed by XRD(X-ray Diffraction). The calcined oyster shell powder was quantitatively analyzed by XRF(X-ray Fluorescence) and the pH of the aqueous solution containing the oyster shell powder calcined at various temperatures was measured using a pH meter.

The physical properties of HAP and HAP-Ag were measured using SEM(Scanning Electron Microscopy), the BET(Brunaurer-Emmett-Teller) Method, and a Porosimeter. An ICP(Inductively Coupled Emission Spectrophotometer) was used to analyze the composition of HAP and HAP-Ag. and a Diode Array Spectrophotometer was used to measure the concentration of the organic adsorbates in the aqueous solution.

3. Results and Discussion

3.1. Physical and Chemical Properties of HAP and HAP-Ag

From the results of the TG/DTA analysis, as shown in Fig. 2, it was found that the oyster shell powder weight started to decrease at 680 ℃ and the exothermic reaction started to occur at 710 ℃. The exothermic peak appeared at 880 ℃, along with a 36.3 % decrease in the powder weight.

The phase change of the oyster shell powder relative to the calcination temperature was analyzed and measured using XRD. The results are summarized in Table 2, where only $CaCO_3$ exited below 700 ℃. As the calcination temperature increased

above 750 ℃, which was a slightly higher temperature than when the exothermic reaction started, the diffraction intensity of CaO increased, while that of $CaCO_3$ decreased. Above 950 ℃, the diffraction of $CaCO_3$ vanished, leaving only that of CaO.

The pH of the 0.1 wt % solution containing the calcined oyster shell powder is summarized in Table 2. Here, the pH of the solution increased along with the phase change from $CaCO_3$ to CaO as the calcination temperature increased. These results indicate that the CaO formed on the calcined oyster shell powder was not reduced to $CaCO_3$, which is characteristic of a strong base. From the above analysis, it was also found that the exothermic peak resulted from the reaction $CaCO_3$ --> CaO + CO_2.

Table 2. pH and phase change of oyster shell powder relative to calcination temperature

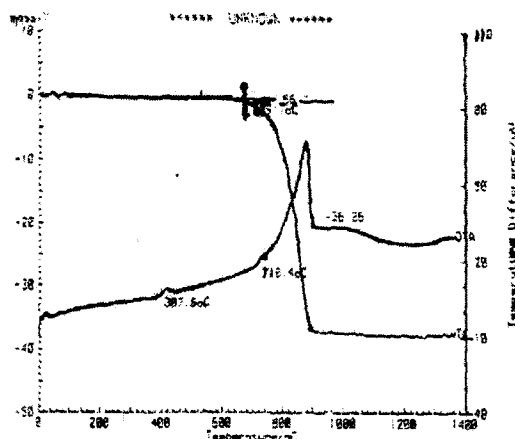| Temperature(℃)	pH	XRD Analysis
650	8.7	$CaCO_3$
750	11.4	$CaCO_3$, CaO
850	12.1	$CaCO_3$, CaO
900-1000	12.7	CaO
1200-1400	13.0	CaO

Fig. 2. TG and DTA curves for oyster shell powder relative to calcination temperature.

Table 3 shows the components of the calcined oyster shell powder above 950 ℃(HAP) analyzed

by XRF. About 99 % of HAP was composed of CaO, while the rest was SiO_2 and Al_2O_3. These are the same major components of zeolite with a molecular structure of $XM_{2/n} \cdot Al_2O_3 \cdot YSiO_2 \cdot ZH_2O$, which is typical inorganic carrier. Consequently, HAP was expected to be exchangeable with an antimicrobial metal ion.

The surfaces of HAP and HAP-Ag were investigated by SEM. As shown in Fig. 3, the diameter of the particles was about $0.5 \sim 15$ μm and the size was not uniform.

Table 3. Quantitative analysis of HAP by XRF

	Average Pore Diameter (Å)	Pore Area (m^2/g)	Bulk Density (g/ml)	Skeletal Density (g/ml)	Porosity (%)
HAP	12844	4.020	0.3865	0.7713	49.89
HAP-Ag	15930	3.013	0.7114	2.0301	64.96

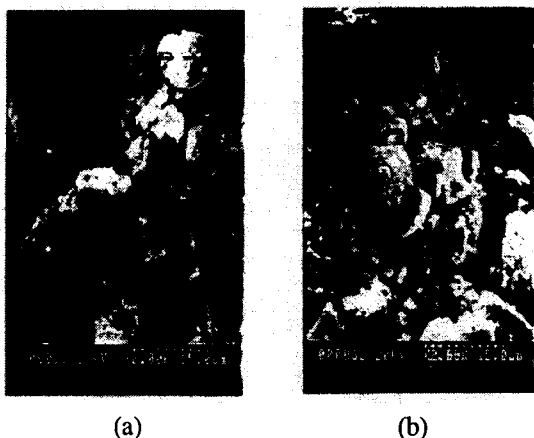(a)   (b)

Fig. 3. Surface of HAP-Ag (a) and HAP (b) photographed by SEM(X2000).

As shown in Figs. 4 and 5, the BET measurement results showed that the specific surface area of HAP(3 m^2/g) was greater than that of HAP-Ag (2 m^2/g).

Table 4 summarizes the density and pore characteristics of HAP and HAP-Ag as measured by a porosimeter. The pore diameters of HAP and HAP-Ag were about 1.3 and 1.6 μm, respectively.

The element compositions of HAP and HAP-Ag were analyzed by ICP and the results are summarized in Table 5. Ca and P were found to

be the main elements in both samples. The Ag content in HAP-Ag was 0.088 %, which was 50 times higher than that in HAP. The higher Ag content in HAP-Ag was due to the silver ion exchange.

To compare the adsorption characteristics of HAP and HAP-Ag with that of $CaCO_3$, 98 % pure $CaCO_3$ was purchased from Aldrich and used as the control. The average diameter of $CaCO_3$ was about 10 μm.
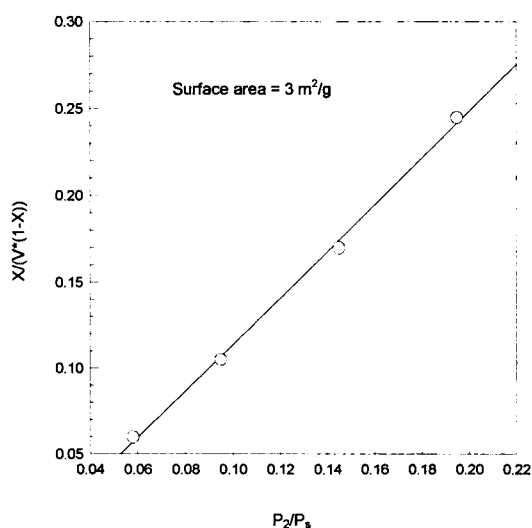

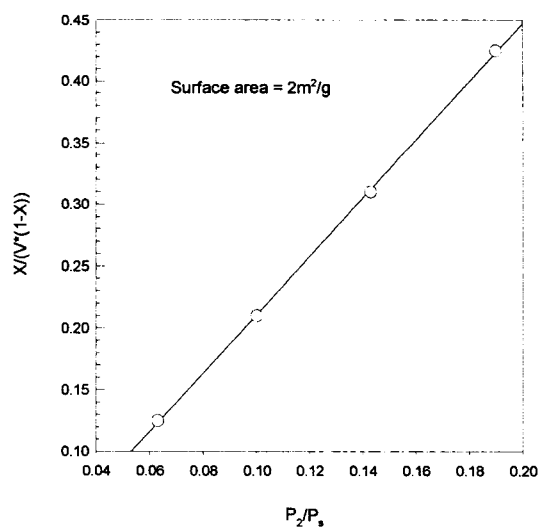Fig. 4. Specific surface area of HAP measured by BET method.

Fig. 5. Specific surface area of HAP-Ag measured by BET method.

Table 4. Pore characteristics of HAP and HAP-Ag measured by Porosimeter

Sample	Element	Wave (nm)	Conc. (ppm)	R.S.D.	Conc.(%)
HAP	Ca	393.366	109	0.85	43.04
	P	214.914	135	0.51	17.03
	Ag	328.068	0.172	0.56	0.0017
	Mg	279.806	18.5	1.5	0.19
	Na	588.995	13.5	0.73	0.14
	Fe	258.588	1.02	1.9	0.010
	Mn	259.373	0.646	0.96	0.0065
	Zn	213.856	0.191	1.3	0.0019
	Sr	338.071	4.61	1.2	0.045
	K	766.490	0.380	1.8	0.0037
	Al	396.152	8.58	0.44	0.083
HAP-Ag	Ca	393.366	94.8	0.64	38.46
	P	214.914	153	0.12	19.89
	Ag	328.068	8.75	1.2	0.088
	Mg	279.806	8.95	1.5	0.090
	Na	588.995	14.1	0.93	0.14
	Fe	258.588	0.956	0.25	0.0097
	Mn	259.373	0.606	1.1	0.0061
	Zn	213.856	0.269	1.5	0.0027
	Sr	338.071	3.61	1.2	0.036
	K	766.490	0.571	3.9	0.0057
	Al	396.152	20.4	0.50	0.20

Table 5. Element analysis of HAP and HAP-Ag by ICP

Component	wt %
SiO_2	1.07
CaO	98.87
Al_2O_3	0.05

3.2. Calibration curves for equilibrium concentration of adsorbates

To measure the adsorbed amount and equilibrium concentration of the adsorbates, calibration curves for the five organic compounds used for the adsorption experiment were obtained using standard solutions. Figs. 6 and 7 show the UV absorbency relative to changes in the concentration of each compound.

The UV absorbency for each organic compound was measured using a Diode Array Spectrophotometer and the measurement conditions are summarized in Table 6. The UV absorbency was measured at lower pH values than the pKa values for each compound shown in Table 1 in order to

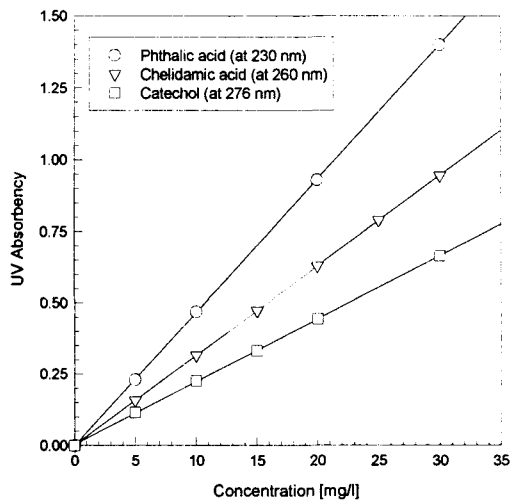measure the absorbency for neutral molecules.

Fig. 6. Calibration curves of phthalic acid, chelidamic acid, and catechol.
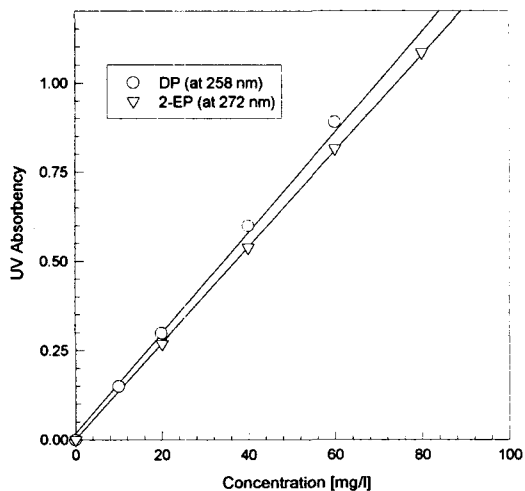

Fig. 7. Calibration curves of DP and 2-EP.

Table 6. Measurement conditions of UV absorbency for each organic compound

Compound	pH	Wavelength (nm)	Absorbency Coefficient ($mg^{-1}cm^{-1}$)
Phthalic Acid	1.5-2.0	230	0.01219
Chelidamic Acid	1.5-2.0	260	0.03148
Catechol	3.5-4.0	276	0.0219
2-Ethyl Phenol	3.5-4.0	272	0.01344
DP	6.0	260	0.01471

3.3. pH of solutions before and after adsorption experiment

The pH of the solutions containing the adsorbates before and after the adsorption experiment was measured as summarized in Table 7. The pH of the solutions containing only adsorbates was within a neutral and acidic range. The increase in the pH of the solutions after the adsorption experiment was due to the existence of the adsorbents and the production of OH⁻ from the following reactions of the adsorbents in the aqueous solution.
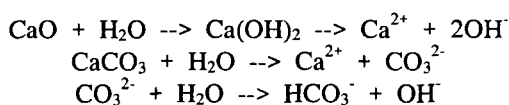
$$CaO + H_2O \longrightarrow Ca(OH)_2 \longrightarrow Ca^{2+} + 2OH^-$$
$$CaCO_3 + H_2O \longrightarrow Ca^{2+} + CO_3^{2-}$$
$$CO_3^{2-} + H_2O \longrightarrow HCO_3^- + OH^-$$

Table 7. pH of adsorbate solutions before and after adsorption

Adsorbate	pH of Adsorbate Solution (100mg/l)	pH of Adsorbate Solution relative to Adsorbent after Adsorption		
		HAP	HAP-Ag	CaCO₃
Phthalic Acid	3.39	12.4	9.53	6.75
Chelidamic Acid	3.37	12.45	9.21	7.5
Catechol	5.9	12.41	9.13	6.74
DP	6.26	12.45	9.3	7.31
2-EP	7.56	12.52	9.87	-

3.4. Adsorption Results

The adsorption equilibrium data was obtained from a batch adsorption experiment. With HAP, HAP-Ag, and CaCO₃, as the adsorbents, equilibrium concentrations were measured for the five organic compounds used as adsorbates. The adsorption uptake(q) relative to the equilibrium concentration(C) was graphed for all the adsorbates and adsorbents, as shown in Figs. 8, 9, 10, 11, 12, 13, and 14. These data were fitted to a Langmuir adsorption isotherm to obtain the Langmuir isotherm constant(b) and adsorption capacity(q_m). The Langmuir parameter values obtained are summarized in Table 8.

As shown in Figs. 8 and 9, with HAP, the adsorbed amount of phthalic acid and chelidamic acid increased further with an increase in the

equilibrium concentration. With HAP-Ag, the adsorption of phthalic acid and chelidamic acid was saturated at an equilibrium concentration of 40 and 20 mg/l, respectively, and for CaCO₃, it was saturated at a concentration of 40 mg/l. As seen in Table 8, the adsorption capacity(q_m) of phthalic acid and chelidamic acid was 2.68 and 1.82 with HAP, which was much greater than the 0.0765 and 0.142 with HAP-Ag, and 0.0706 and 0.0708 with CaCO₃, respectively. The higher amount of adsorption with HAP than with HAP-Ag would appear to be due to the fact that exchanged silver ion decreased the adsorption sites on HAP-Ag. The adsorption data for both HAP and HAP-Ag fitted well to a Langmuir isotherm.

More catechol was adsorbed to HAP than to HAP-Ag at an equilibrium concentration of below 15 mg/l, as shown in Fig. 10. However, the overall adsorption amount was greater for HAP-Ag than HAP. The adsorption capacity of HAP-Ag was 2.58, which was greater than the 0.73 for HAP and 0.22 for CaCO₃. This was attributed to the fact that the OH⁻ functional group of catechol interacted more effectively with the Ag^+ on HAP-Ag than the Ca^{2+} on HAP.

As shown in Fig. 11, the adsorption of DP was saturated at an equilibrium concentration of about 30 mg/l for all the adsorbents, HAP, HAP-Ag, and CaCO₃. The adsorption capacity of HAP was

Table 8. Langmuir parameter values

| Adsorbate	Adsorbent	a(=q_mb)	b	q_m
Phthalic Acid	HAP	0.0319	0.0050	2.68
	HAP-Ag	0.0071	0.0926	0.0765
	CaCO₃	0.0132	0.1863	0.0706
Chelidamic Acid	HAP	0.0658	0.0362	1.82
	HAP-Ag	0.0478	0.3367	0.142
	CaCO₃	0.0030	0.0419	0.0708
Catechol	HAP	0.0542	0.0747	0.73
	HAP-Ag	0.0327	0.0126	2.58
	CaCO₃	0.0017	0.0078	0.22
DP	HAP	0.0548	0.2881	0.19
	HAP-Ag	0.0075	0.0804	0.094
	CaCO₃	0.0041	0.0627	0.065
2-EP	HAP	0.0010	0.0118	0.087
	HAP-Ag	0.0013	1.3×10^{-10}	-
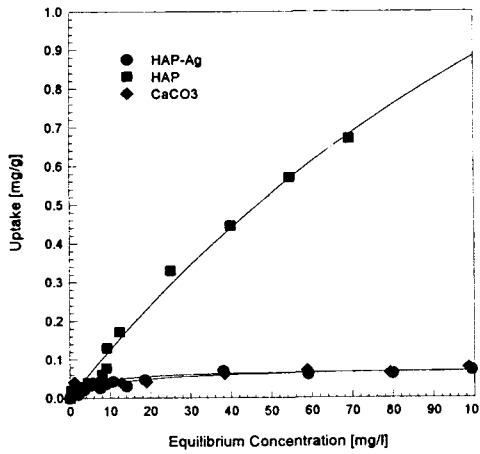
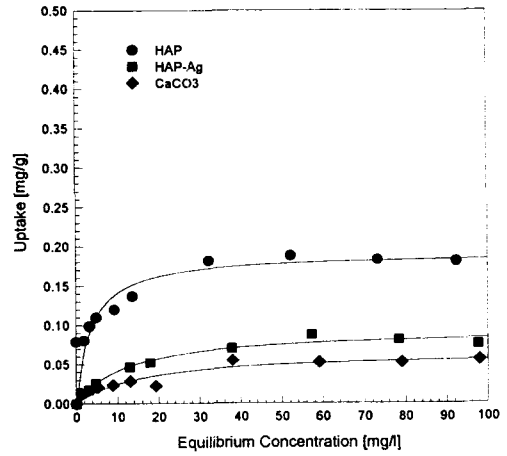Fig. 8. Adsorption of phthalic acid onto HAP, HAP-Ag, and CaCO₃.

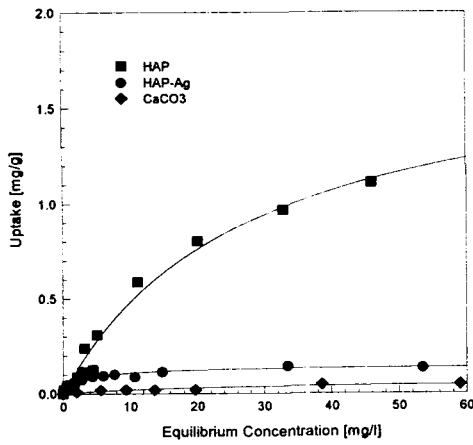Fig. 11. Adsorption of DP onto HAP, HAP-Ag, and CaCO₃.

Fig. 9. Adsorption of chelidamic acid onto HAP, HAP-Ag, and CaCO₃.
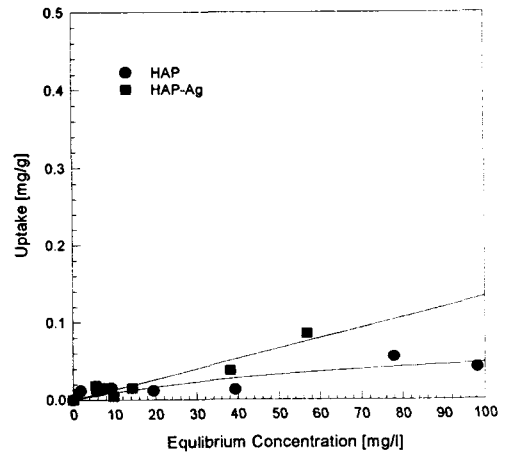
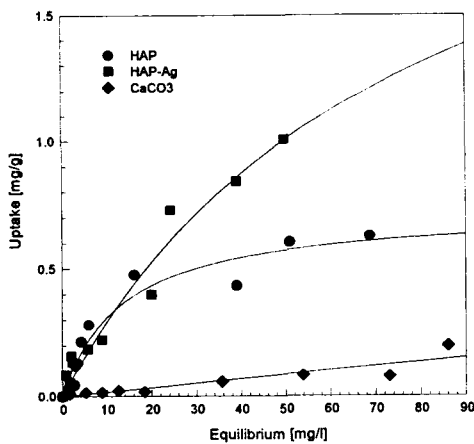Fig. 12. Adsorption of 2-EP onto HAP and HAP-Ag.

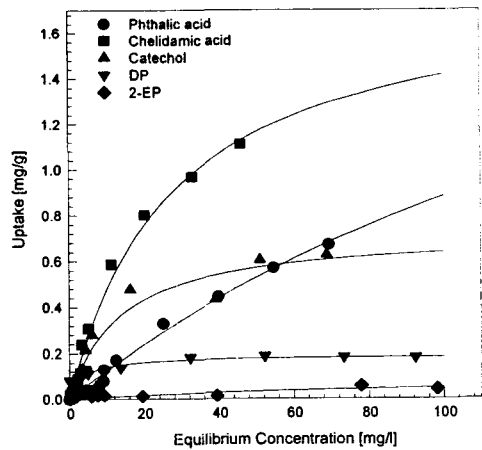Fig. 10. Adsorption of catechol onto HAP, HAP-Ag, and CaCO₃.

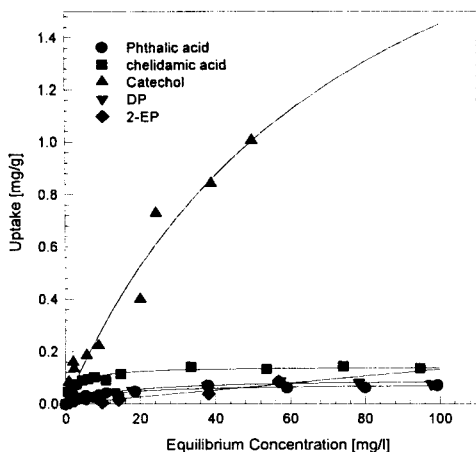Fig. 13. Adsorption of five organic compounds onto HAP.

Fig. 14. Adsorption of five organic compounds onto HAP-Ag.

0.19, which was greater than the 0.094 for HAP-Ag and 0.065 for CaCO₃.. The adsorption amount of DP with HAP was almost twice that with HAP-Ag. These results would appear to be due to the fact that the cationic surfactant DP has a cationic exchange capacity of two in proportion to the oxidation number of Ca^{2+} and one with Ag^+.

As shown in Figs. 8, 9, 10, and 11, the adsorption capacities of the organic compounds with CaCO₃ were smaller than those with HAP and HAP-Ag, except for DP. The adsorption amount per gram of adsorbent was in the sequence of catechol > phthalic acid > DP > chelidamic acid.

Fig. 12 shows that the adsorbed amount of 2-EP was very small both with HAP and HAP-Ag. The adsorption capacity of 2-EP was also found to be very small, as seen in Table 8. It is believed that the ethyl group in the 2-EP structure inhibits the interaction of OH⁻ with adsorbents, thereby causing only a small amount of adsorption of 2-EP.

Fig. 13 shows the adsorption trends of all five organic compounds onto HAP. The adsorption amount per gram of adsorbent was in the sequence of chelidamic acid > phthalic acid > catechol > DP > 2-EP. At an equilibrium concentration of below 50 mg/l, the adsorption amount of catechol was greater than that of phthalic acid.

With HAP-Ag, the adsorption amount of catechol was almost 10 times that of the others, as seen in Fig. 14. This result would appear to be due to the effective interaction of two OH⁻ groups with the HAP-Ag structure. The adsorption amount

per gram of adsorbent was in the sequence of catechol > chelidamic acid > phthalic acid > DP > 2-EP.

4. Conclusions

When HAP and HAP-Ag were used as adsorbents in an adsorption experiment, the pH of the solution increased as a result of the production of OH⁻ ions from the interaction of CaO with H₂O. Consequently, it was found that the adsorption amount of organic compounds able to combine with Ca^{2+} ions is greater than those of phenolic compounds and cationic surfactants.

The pKa of organic compounds, such as phthalic acid and chelidamic acid, is about 3 to 4, which was lower than the pH of the solution containing HAP and HAP-Ag. As such, since the organic compounds seemingly existed in an ionic state in the solution during adsorption, they could be adsorbed well to the adsorbents by ion exchange, electrostatic forces, and chelation. The greater adsorption onto HAP than HAP-Ag was apparently due to the fact that the silver ion positioned on HAP-Ag by ion exchange decreased the number of adsorption sites.

The greater adsorption of catechol was seemingly caused by the electrostatic force and chelation of two OH⁻ functional groups with the metal ions on the surface of the adsorbents. In particular, catechol exhibited a good adsorption affinity for the silver ion on the surface of HAP-Ag.

2-EP showed a relatively poor adsorption compared to the other adsorbates. This was attributed to the fact that the ethyl group in the 2-EP structure may inhibit the interaction of the OH⁻ group with the adsorbents.

DP was adsorbed more than 2-EP onto the adsorbents because of a cationic exchange with the metal ions on the surface of the adsorbents and hydrophobic bonding with long carbon chains.

The adsorption affinities of the adsorbates were in the sequence of chelidamic acid > phthalic acid > catechol > DP > 2-EP with HAP and catechol > chelidamic acid > phthalic acid > DP > 2-EP with HAP-Ag. All the adsorption data fitted well to a Langmuir adsorption isotherm.

Since the specific surface areas of HAP and HAP-Ag were larger and the pHs of the solutions

higher than those of $CaCO_3$, more organic acids and catechol could be adsorbed to HAP and HAP-Ag. In addition, the adsorption amount per unit area was about 0.3 mg/m^2, which is comparable to that of other common adsorbents. Accordingly, if the specific areas of HAP and HAP-Ag could be further increased, this would clearly provide a cost effective method for the removal of organic compounds.

References

[1] Kim, M. P. and J. D. Han, 1997, "Adsorption properties of oyster shell powder as landfill cover", J. of Korean Society of Environmental Engineers., 19, 97~110.

[2] Song, D. G. , J. K. Kim, and N. C. Seong, 1997, Proc. of Korean Society of Environmental Engineers., 359~362.

[3] Shin, C. H., B. I. Noh, and M. C. Jo, 1997, "Development of water treatment agent with adsorption and antimicrobial activity using oyster shell", Final Project Report for Department of Agriculture Fishery, Pusan, Korea.

[4] Jo, M. C., B. I. Noh, and C. H. Shin, 2,000, "Reuse of oyster shell waste as antimicrobial water treatment agent by silver ion exchange", J. of Korean Society of Environmental Engineers., 4, 185~193.

[5] Stevenson, F. J., 1994, Humus Chemistry, 2nd Ed., John Wiley & Sons, Inc.

[6] Kenneth, E., N. V. Gounaris, and W. S. Hou, 1992, Adsorption Technology for Air and Water Pollution Control., Lewis Publishers, Inc.

[7] Yamamoto, T., S. Uchida, and Y. Kurihara, 1991, "Disinfection of zeolite containing metal ion", J. of Antibact. Antifungi Agents, 19, 425~431.

[8] Handbook of Chemistry and Physics, 1987, 67th Edn., CRC Press, Inc.